

Pulsation in λ Bootis stars^{*}

E. Paunzen¹, W.W. Weiss¹, R. Kuschnig¹, G. Handler¹, K.G. Strassmeier¹, P. North², E. Solano³, M. Gelbmann¹, M. Künzli², and R. Garrido⁴

¹ Institut für Astronomie der Universität Wien, Türkenschanzstrasse 17, A-1180 Wien, Austria (last_name@astro.ast.univie.ac.at)

² Institut d'Astronomie de l'Université de Lausanne, CH-1290 Chavannes-des-Bois, Switzerland (Pierre.North@obs.unige.ch)

³ INSA; ESA IUE Observatory, P.O. Box 50727, E-28080 Madrid, Spain (esm@vilspa.esa.es)

⁴ Instituto de Astrofísica de Andalucía, CSIC, P.O. Box 3004, E-18080 Granada, Spain (garrido@iaa.es)

Received 11 December 1997 / Accepted 31 March 1998

Abstract. In this paper we present a further step in applying asteroseismic techniques to the group of λ Bootis stars which can be characterized as nonmagnetic A to F-type Population I dwarfs with significant (surface) underabundances of Fe-peak elements. Since no conclusive theory explaining the origin of the observed abundance anomalies exists, an extensive photometric survey for pulsation in this group has been initiated. Knowledge about the pulsational properties (most members are located within the classical instability strip) could help to establish constraints about the overall abundance of these stars as well as on the evolutionary status.

New photometric observations were carried out for eleven stars. Variability was detected in four stars (e.g. λ Bootis itself) whereas the remaining seven objects are probably constant.

In total, 52 members of this group have been photometrically investigated so far. With 22 pulsating and 30 “constant” stars, we derive a ratio of at least 50% for variable to nonvariable members *inside* the classical instability strip. This result is based on high quality Hipparcos and new photometric data.

The observed $\log \bar{\rho}/\bar{\rho}_{\odot}$ and $\log P$ values for the pulsating members are compatible with standard (solar abundant) δ Scuti models supporting the hypothesis that the found abundance anomalies are restricted to the surface only. Otherwise the pulsational properties of this group are not outstanding compared to “normal” δ Scuti stars, indicating that the mechanism driving the pulsations is very similar.

Key words: stars: early type – stars: oscillations – stars: variables: δ Sct

1. Introduction

Since the discovery of pulsating stars, asteroseismic tools have been applied successfully to a wide variety of different objects. Significant advances in both observation and theory are produc-

Send offprint requests to: E. Paunzen

^{*} Based on observations obtained at ESO-La Silla, CTIO, SAAO, McDonald Observatory, Instituto Astrofísica Andalucía Observatory and with the Hipparcos satellite

ing better astrophysical descriptions of all classes of multiperiodic pulsators such as the δ Scuti variables. Information about the global and atmospheric properties of these stars helped to understand the stellar and chemical evolution in the H-R diagram. The evolutionary status, and information about the chemical composition, are very much needed for the λ Bootis stars.

The λ Bootis stars are nonmagnetic chemically peculiar stars (Population I, A- to F-type dwarfs) whose spectra show significant underabundances of metals (with the exceptions of C, N, O and S). The origin of the λ Bootis phenomenon remains controversial. There are currently two main competing theories: mass loss coupled with diffusion (Michaud & Charland 1986) and accretion of interstellar material (Venn & Lambert 1990). The latter model requires that λ Bootis stars are very close to the Zero-Age Main Sequence (Turcotte & Charbonneau 1993), whereas the other one produces evolved λ Bootis stars, so an independent determination of the age and evolutionary state of these stars could resolve the debate about the two scenarios. The original diffusion/mass-loss theory was challenged by Charbonneau (1993) who showed that even a moderate amount of rotationally induced mixing is sufficient to prevent the deep chemical separation required to produce underabundances at later times of the stellar evolution. Both theories are discussed in more detail by Paunzen et al. (1997a).

In a first attempt to describe the pulsational behaviour a ratio of at least 50% for variable to nonvariable members of this group inside the classical instability strip was determined (Paunzen et al. 1997b). As a further step we present a statistical analysis of the pulsating λ Bootis stars using the Hipparcos and improved photometric data.

2. Program stars and observations

All presented program stars for our photometric survey were taken from Renson et al. (1990), Paunzen et al. (1997a) and Paunzen & Gray (1997). Results of probably “constant” stars have been published by Paunzen et al. (1997b). A series of IBVS notes was dedicated to the pulsating members of this group. The following observations are presented for the first time and the results are reviewed in more detail:

HD 23392, HD 36726, HD 64491, HD 84123, HD 101108,

Table 1. Observations' log of four newly discovered pulsating λ Bootis stars, the differential light curves are shown in Figs. 1 and 2.

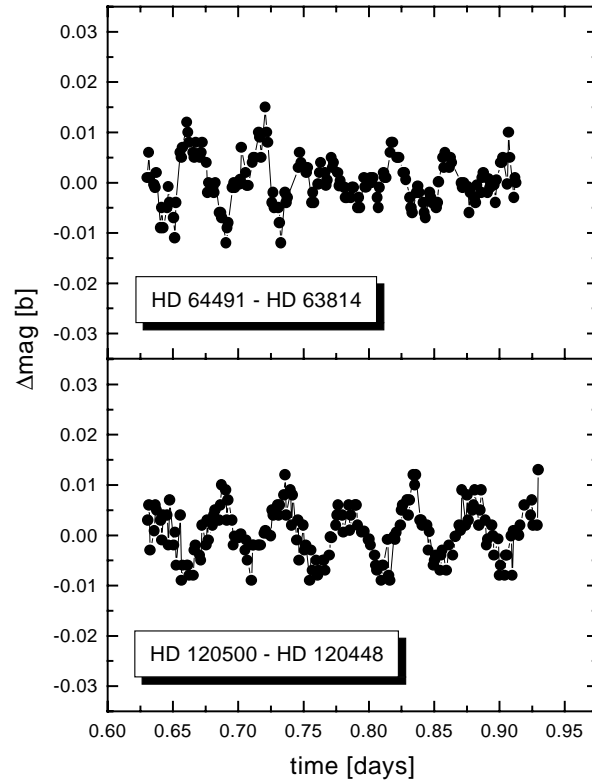
HD	JD	hrs	m_V [mag]	Spec.	Per. [min]	Amp. [mag]
64491	2450481	6.8	6.2	λ Bootis	71	0.009
	2450482	6.8				
66682			7.1	F2		
63814			7.0	F8		
105058	2450864	1.8	8.9	λ Bootis	58	0.003
105123			7.8	F5		
105458			7.9	A5		
120500	2450569	7.3	6.6	λ Bootis	70	0.011
	2450570	7.2				
120448			6.8	A0		
120317			6.6	F2		
125162	2450868	1.9	4.2	λ Bootis	33	0.003
	2450873	3.8				
	2450874	2.7				
126660			4.1	F7 V		
129002			5.4	A1 V		

Table 2. Observations' log of seven constant λ Bootis stars. HD 23392, HD 36726, HD 84123, HD 101108 and HD 106223 were observed at the APT, HD 290799 and HD 294253 with the 70cm Swiss telescope at ESO-LaSilla

HD	JD	hrs	m_V [mag]	Spec.	Limit [mmag]
23392	2450823	5.0	8.7	λ Bootis	2 [b]
	2450825	4.5			
23504			8.1	B9	
36726	2450825	6.4	8.8	λ Bootis	3 [b]
	2450826	2.9			
36709			8.3	A0	
36760			7.6	B7V	
84123	2450485	5.3	6.9	λ Bootis	3 [b]
84388			7.8	F2	
101108	2450874	8.4	8.9	λ Bootis	2 [b]
	2450875	8.2			
	2450876	7.9			
100215			8.0	Am	
100311			7.9	A3 V	
106223	2450876	8.2	7.4	λ Bootis	3 [b]
	2450877	7.9			
105388			7.5	A0 V	
106152			7.8	F7	
290799	2450423	4.7	10.6	λ Bootis	10 [V]
294253			9.7	λ Bootis	7 [V]
35640			6.3	B9V	
36058			6.4	B9	

HD 106223 and *HD 120500*: These stars were observed with one of the University of Vienna automatic photoelectric telescopes (APT). For a detailed description of this instrument see Strassmeier et al. (1997). A typical integration time of 15 seconds in Strömgen *v* and *b* was chosen.

HD 64491 and HD 120500 were found to be variable. The differential light curves for both stars are shown in Fig. 1. All data

**Fig. 1.** Differential light curves of HD 66491 (upper panel) and HD 120500 (lower panel) for one night in Strömgen *b*.

sets were analyzed using a standard Fourier technique (Paunzen et al. 1998b). The observations' log, comparison stars used as well as the determined periods and peak-to-peak amplitudes of the pulsation are listed in Table 1.

HD 23392, HD 36726, HD 84123, HD 101108 and HD 106223 proved to be constant with the upper levels (for the definition of these limits see Paunzen et al. 1997b) listed in Table 2.

HD 105058 and *HD 125162*: Photometric observations were obtained in four nights with the 90cm telescope of McDonald Observatory with an integration time of 10 seconds in Johnson *B* (HD 105058) and Strömgen *v* (HD 125162; Table 1). For the light curves in Fig. 2, the data were averaged to a time resolution of 60 seconds. Please note the very low amplitude of the pulsation and the high quality of the data (rms \approx 0.8 mmag). HD 125162 (λ Bootis itself) was reported as constant by Paunzen et al. (1997b) with an upper limit of 6.6 mmag. The new observations resulted in a period of 33 minutes and a peak-to-peak amplitude of 3 mmag. Multiperiodic behaviour for HD 105058 and HD 125162 is evident (Fig. 2).

HD 290799 and *HD 294253*: Observations were performed during the night of 06/07.12.96 on the 70cm Swiss-telescope at ESO, La Silla, with the Geneva P7 photometer. HD 35640 ($V=6.3$; B9V) and HD 36058 ($V=6.4$, B9) were used as comparison stars. Both program stars proved to be constant with an upper limit of 10 mmag (HD 290799) and 7 mmag (HD 294253) in Geneva *V*.

Table 3. Pulsating λ Bootis stars. An asterisk denotes stars without Hipparcos parallaxes. The errors are given in units of the last digit of the corresponding quantity.

HD	$b - y$ (± 0.007)	$\log T_{\text{eff}}$ (± 0.010)	$\log g$ (± 0.1)	M_V [mag]	$B.C.$ [mag]	$\log L/L_{\odot}$	$\log P$ (± 0.05)	Amp. [mmag]	$\log \bar{\rho}/\bar{\rho}_{\odot}$ (± 0.05)	Ref.
6870	0.153	3.869	4.0	2.54(13)	-0.10	0.92(4)	-1.19	30 [V]	-0.68	BR79
11413	0.108	3.903	3.8	1.57(11)	-0.13	1.32(4)	-1.43	18 [B-V]	-1.01	WA83
30422	0.101	3.903	4.2	2.38(9)	-0.13	1.00(3)	-1.68	10 [b]	-0.45	KU96
64491	0.196	3.851	4.1	2.32(12)	-0.09	1.01(4)	-1.31	9 [b]	-0.66	
75654	0.161	3.869	3.8	1.92(10)	-0.10	1.17(4)	-1.06	20 [V]	-1.01	BA77
83041	0.252	3.839	3.3	2.06(50)	-0.11	1.12(20)	-1.18	7 [b]	-1.54	PA96a
84948B*	0.196	3.822	3.7	1.50(30)	-0.11	1.34(12)	-1.11	15 [v]	-1.26	PA98a
102541	0.163	3.886	4.1	2.46(27)	-0.10	0.96(11)	-1.30	30 [v]	-0.57	KU97
105058	0.129	3.887	4.4	2.52(42)	-0.10	0.93(16)	-1.40	3 [b]	-0.25	
109738*	0.165	3.881	3.8	1.60(30)	-0.10	1.50(12)	-1.49	10 [b]	-1.15	PA95c
111786	0.161	3.881	3.9	2.24(10)	-0.10	1.04(4)	-1.49	8 [b]	-0.82	KU94a,PA98b
120500	0.069	3.924	3.9	0.82(28)	-0.16	1.64(11)	-1.32	11 [b]	-1.03	
125162	0.051	3.940	3.9	1.81(4)	-0.17	1.24(2)	-1.64	2 [b]	-0.80	
142703	0.180	3.863	3.9	2.49(9)	-0.10	0.94(3)	-1.20	6 [b]	-0.80	PA94a;95b;96b
142994*	0.199	3.845	3.5	0.80(30)	-0.10	1.62(12)	-0.80	38 [b]	-1.58	PA95b;98b,WE94
168740	0.136	3.892	3.9	1.87(11)	-0.12	1.20(4)	-1.44	16 [b]	-0.88	PA95d
168947*	0.172	3.875	3.6	1.10(30)	-0.10	1.50(12)	-1.23	26 [V]	-1.36	PA94b
183324	0.051	3.968	4.2	1.94(11)	-0.24	1.22(4)	-1.68	4 [v]	-0.43	KU94b
191850*	0.166	3.869	3.7	1.50(30)	-0.10	1.30(12)	-1.13	34 [b]	-1.17	PA95a
192640	0.101	3.903	4.0	1.86(5)	-0.13	1.21(2)	-1.58	26 [b]	-0.76	KS96,PA96b
210111	0.136	3.881	3.8	1.89(15)	-0.10	1.18(5)	-1.45	8 [V]	-0.99	PA94c
221756	0.056	3.954	3.9	1.28(10)	-0.20	1.47(4)	-1.36	7 [b]	-0.89	PA96a

Ref. . . . Reference on the pulsational properties (column “log P ” and “Amp.”) can be found bold-faced in the bibliography (AA##a; A,a...letter, number)

3. Calibrations

For a statistical analysis of the pulsational properties for this group, we located the program stars in a $(b - y)$ vs. M_V (Diagram 1 hereafter) and/or $\log T_{\text{eff}}$ vs. $\log L/L_{\odot}$ diagram (Diagram 2 hereafter). Strömgren colours for the program stars were taken from Hauck & Mermilliod (1990), Gray & Olsen (1991) and Handler (1995). The M_V values were derived from the Hipparcos parallaxes. Photometrically determined M_V values (following Paunzen et al. 1997b) were used for HD 36726, HD 109738, HD 142994, HD 143148, HD 168947, HD 191850, HD 290799 and HD 294253 because no Hipparcos parallaxes are available. Fig. 3 shows Diagram 1 with the observational borders of the instability strip taken from Breger (1979).

As a further step, we have derived $\log T_{\text{eff}}$ and $\log L/L_{\odot}$ values for all program stars. The determination of the effective temperature (and the error estimation) is based on the calibration given by Napiwotzki et al. (1993). For the two spectroscopic binary systems HD 84948 and HD 171948 spectroscopically determined values from Paunzen et al. (1998a) were used. The absolute bolometric magnitude M_{bol} was computed by using the absolute magnitudes M_V and adding the bolometric corrections taken from Schmidt-Kaler (1982). With $M_{\text{bol}(\odot)} = 4.75$ (cgs units are assumed throughout) given by Cayrel de Strobel (1996), we have calculated $\log L/L_{\odot}$ (Tables 3 and 4). Fig. 4 shows Diagram 2 with Main Sequence evolutionary tracks (Claret 1995) and the observational borders of the instability strip (Breger 1995).

4. Results

In total, 52 program stars (Tables 3 and 4) were observed photometrically. We had to exclude HD 192424 (probably constant) from our further conclusions since neither photometric (Geneva and Strömgren) colours nor a Hipparcos parallax are available. The following six (variable) λ Bootis stars deserve further interest:

HD 83041: a very cool λ Bootis star outside the classical instability strip (4σ in $b - y$) in Diagram 1. Since its position within Diagram 2 is only 1σ outside the cool border, we tend to believe that reddening is affecting the observed colours.

HD 188324 and *HD 221756*: Both stars seem to lie beyond the hot border of the instability strip (3σ and 2σ in $b - y$ respectively). Spectroscopically determined values for the effective temperature (Stürenburg 1993; U. Heiter, private communication) are in good agreement with the photometrically derived ones. Especially HD 188324 deserves further attention. With a very short period (30 minutes) and a very low surface metallicity ($[Z] \approx -1.5$), it seems to be quite outstanding compared to the other pulsating λ Bootis stars.

HD 111786, *HD 142994* and *HD 192640*: These three stars were targets of multisite campaigns. Results have been reported in Paunzen et al. (1998b; HD 111786 and HD 142994) and Kusakin & Mkrtchian (1996; HD 192640). We have only considered the period with the highest amplitude for our further investigations.

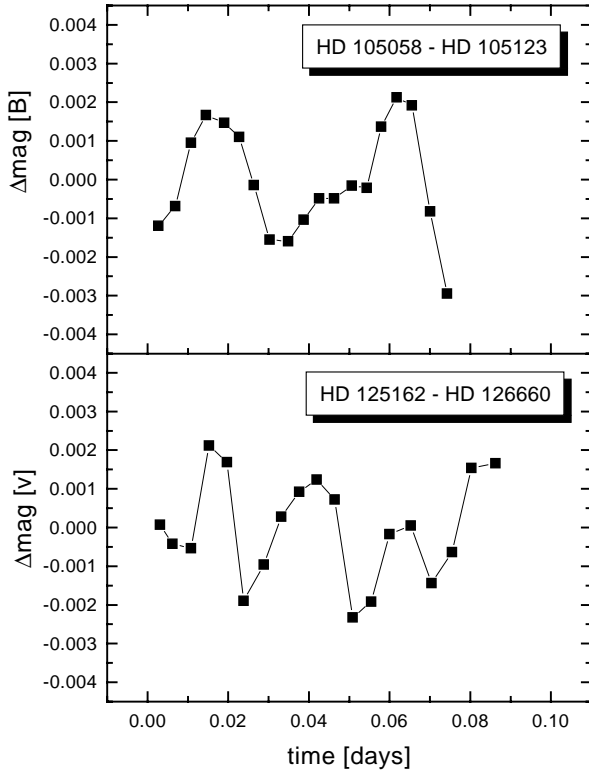


Fig. 2. Differential light curves of HD 105058 (Johnson B ; upper panel) and HD 125162 (Strömgren v ; lower panel) for one night.

First of all, the ratio of variable to nonvariable λ Bootis stars inside the classical instability strip was derived. Our first attempt (Paunzen et al. 1997b) resulted in the conclusion that at least 50% of all investigated λ Bootis stars inside the instability strip are variable. With the new Hipparcos parallaxes and thus more precisely known luminosities as well as further observational data, a proof of our prior results should be possible. We have used Diagrams 1 and 2 to perform this analysis. The latter is depending on calibrations (derived from “standard” stars with solar abundance) and therefore more uncertain than direct observations ($b - y$ and parallax). In order to test all possible cases within the error bars, the introduction of five “scenarios” for measurements inside the instability strip (note that the borders of the classical instability strip cannot be treated as strict) seems appropriate:

- Case 1: all measurements are treated without error bars
- Case 2: all measurements which could be located inside the instability strip within the error bars are counted
- Case 3: all measurements which could be located outside the instability strip within the error bars are *not* counted
- Case 4: “worst case”, Case 3 only for variable stars and Case 2 for nonvariable stars
- Case 5: “best case”, Case 3 only for nonvariable stars and Case 2 for variable stars

Table 5 lists the percentages for all proposed cases. If one takes the “observational” parameters ($b - y$ and M_V), the worst case yields 49% pulsating stars whereas the best case gives 69%. Tak-

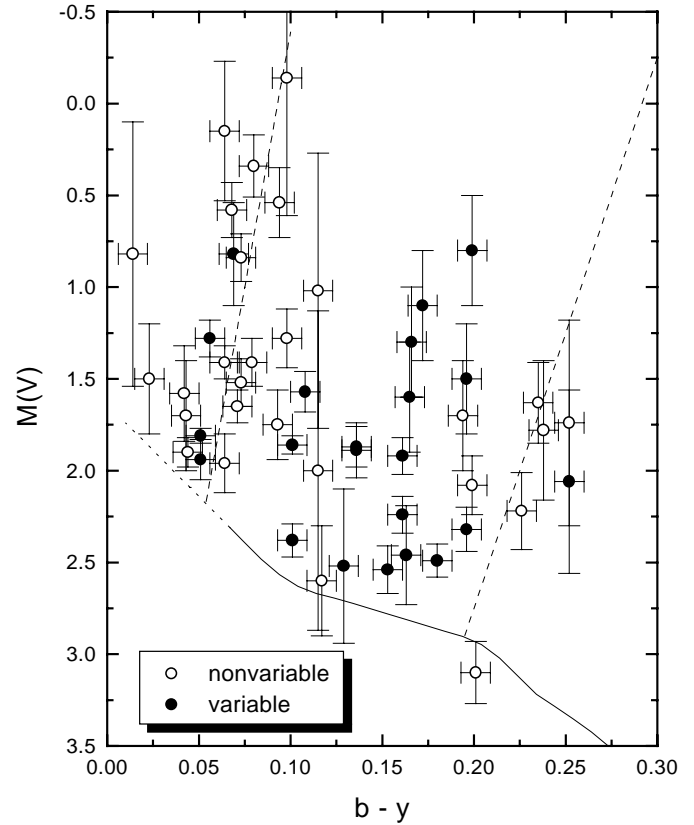


Fig. 3. The location of λ Bootis stars in a $(b - y)$ vs. M_V diagram. The Zero-Age Main Sequence is taken from Crawford (1979), the borders of the instability strip are from Breger (1979). The error bars are according to Table 3 and 4.

ing the average of all five cases, we derive $\frac{\#(var)}{\#(nonv)} = 0.58(9)$ for the “observational” as well as for the “calibrated” parameters.

We therefore conclude that the ratio of variable to nonvariable λ Bootis stars *inside* the classical instability strip is at least 50% supporting prior investigations. This conclusion is based on a sample of 51 program stars as well as on high quality Hipparcos parallaxes.

Based on our sample of pulsating λ Bootis stars (Table 3) a statistical analysis of the pulsation behaviour was made. The mean density of the pulsating members has been computed according to the formula:

$$\log \bar{\rho} / \bar{\rho}_{\odot} = \log g - 0.5 \log L / L_{\odot} + 2 \log T_{\text{eff}} - 11.96$$

This quantity is independent of an age and mass determination but still depends on the photometric calibration in the Strömgren system ($\log g$ and $\log T_{\text{eff}}$). In order to compare the determined mean densities with those of “normal” (solar abundant) δ Scuti stars, the Q-values for *radial* pulsation modes from Stellingwerf (1979) were used. With the relation $P = Q \sqrt{\bar{\rho} / \bar{\rho}_{\odot}}$, lines of constant Q for the fundamental and several overtones were computed. Fig. 5 shows the derived location of all pulsating λ Bootis stars within a $\log \bar{\rho} / \bar{\rho}_{\odot}$ vs. $\log P$ diagram.

Similar to the classical δ Scuti stars (Breger 1979), fundamental and overtone modes seem to be excited. It is encouraging

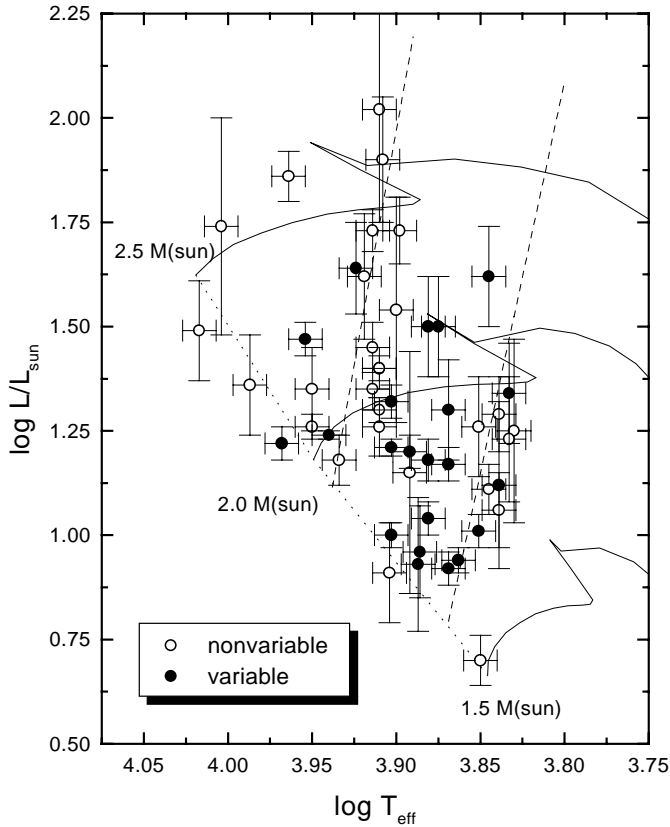


Fig. 4. The location of λ Bootis stars in a $\log T_{\text{eff}}$ vs. $\log L/L_{\odot}$ diagram. The borders of the instability strip are from Breger (1995) with the evolutionary tracks and the Zero-Age Main Sequence from Claret (1995). The error bars are according to Tables 3 and 4.

to see that *no* program star exhibit a $\log P$ value which is larger than the corresponding value for the fundamental mode. The pulsation frequencies of λ Bootis stars are obviously compatible with *solar abundant* models. This result strengthens further the hypothesis that the observed abundance pattern is restricted to the surface and is not representative for the stellar interior. Furthermore, we conclude that the mechanism driving the pulsation of both groups is very similar.

5. Conclusions

We have discussed new photometric observations for eleven λ Bootis stars. Four of them turned out to be variable such as λ Bootis itself.

In total, 51 program stars have been used to analyze the pulsation properties of λ Bootis stars. Using observational ($b - y$ vs. M_V) and calibrated ($\log T_{\text{eff}}$ vs. $\log L/L_{\odot}$) diagrams, we derived a ratio of variable to nonvariable members inside the classical instability strip of at least 50%. This result is in accordance with an earlier investigation based on a smaller sample.

The location of all known pulsating program stars in a $\log \bar{\rho}/\bar{\rho}_{\odot}$ vs. $\log P$ diagram is consistent with those of (*solar abundant*) δ Scuti stars which supports the hypothesis that the λ Bootis abundance pattern (underabundance of Fe-peak elements) is restricted to the stellar surface. This conclusion is

Table 4. Nonvariable λ Bootis stars, an asterisk denotes stars without Hipparcos parallaxes ($\sigma(b - y) = \pm 0.007$; $\sigma(\log T_{\text{eff}}) = \pm 0.010$). The errors are given in units of the last digit of the corresponding quantity.

HD	$b - y$	$\log T_{\text{eff}}$	M_V [mag]	$B.C.$ [mag]	$\log L/L_{\odot}$
319	0.079	3.910	1.41(13)	-0.15	1.40(5)
23392	0.014	4.004	0.82(72)	-0.43	1.74(26)
31295	0.044	3.950	1.80(8)	-0.20	1.26(3)
36726*	0.043	3.987	1.70(30)	-0.34	1.36(12)
38545	0.042	3.950	1.58(26)	-0.20	1.35(10)
66920	0.073	3.919	0.84(13)	-0.15	1.62(5)
74873	0.064	3.934	1.96(16)	-0.17	1.18(6)
79025	0.094	3.898	0.54(19)	-0.12	1.73(8)
81290	0.252	3.830	1.74(56)	-0.11	1.25(22)
82573	0.068	3.914	0.58(18)	-0.15	1.73(5)
83277	0.238	3.833	1.78(38)	-0.11	1.23(15)
84123	0.235	3.839	1.63(22)	-0.11	1.29(9)
91130	0.073	3.914	1.52(13)	-0.15	1.35(5)
101108	0.115	3.892	2.00(87)	-0.12	1.15(29)
106223	0.226	3.839	2.22(21)	-0.11	1.06(9)
141851	0.071	3.910	1.65(9)	-0.15	1.30(3)
143148*	0.194	3.851	1.70(30)	-0.09	1.26(12)
145782	0.080	3.964	0.34(17)	-0.24	1.86(6)
149303	0.064	3.910	1.41(9)	-0.15	1.40(3)
154153	0.199	3.845	2.08(16)	-0.10	1.11(6)
156954	0.201	3.850	3.10(17)	-0.10	0.70(6)
171948		3.954	1.96(18)	-0.20	1.20(8)
179791	0.064	3.908	0.15(38)	-0.15	1.90(15)
188164	0.098	3.914	1.26(16)	-0.15	1.45(6)
193256	0.115	3.900	1.02(75)	-0.12	1.54(27)
193281	0.098	3.910	-0.14(75)	-0.15	2.02(27)
204041	0.093	3.910	1.75(19)	-0.15	1.26(7)
290799*	0.117	3.904	2.60(30)	-0.13	0.91(12)
294253*	0.023	4.017	1.50(30)	-0.48	1.49(12)

Table 5. Ratios of variable to nonvariable λ Bootis stars for all possible cases discussed in the text. The upper panel refers to Diagram 1 (Fig. 3), the lower panel to Diagram 2 (Fig. 4)

	#(var)	#(nonv)	ratio
Case 1	17	14	55%
Case 2	20	19	52%
Case 3	18	9	67%
Case 4	18	19	49%
Case 5	20	9	69%
Case 1	15	11	58%
Case 2	19	16	54%
Case 3	13	8	62%
Case 4	13	16	45%
Case 5	19	8	70%

in agreement with both the diffusion/mass-loss and the diffusion/accretion model and therefore does not allow to discriminate between the two scenarios. The possibly excited modes range from the fundamental mode up to high overtones. In respect to pulsation, we do not find a difference between the group of λ Bootis and δ Scuti stars.

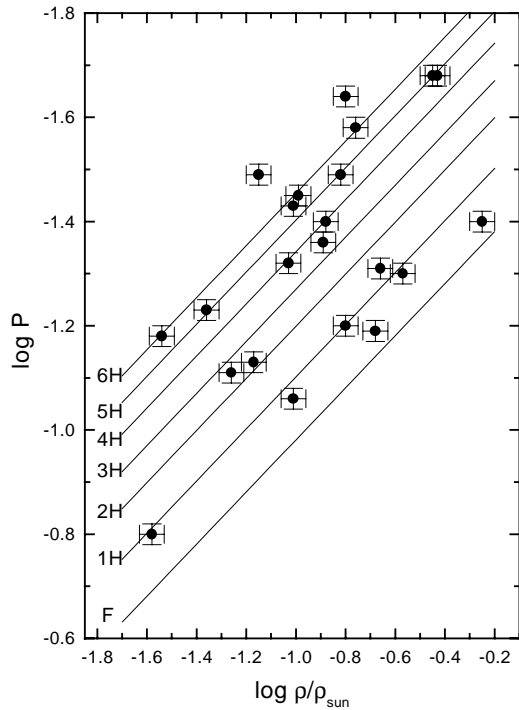


Fig. 5. The pulsating λ Bootis stars from Table 3 in a $\log \bar{\rho}/\bar{\rho}_{\odot}$ vs. $\log P$ diagram. The $\log Q$ values for the different *radial* modes were taken from Stellingwerf (1979).

Acknowledgements. This research was carried out within the working group *Asteroseismology-AMS* with funding from the Fond zur Förderung der wissenschaftlichen Forschung (FWF), project *S7303-AST* and was partly supported by the Swiss Fonds National de la Recherche Scientifique. KGS acknowledges support by the FWF, project *S7301-AST*, GH acknowledges support by the FWF, project *S7304-AST*. We would like to thank P. Charbonneau for helpful comments. Use was made of the Simbad database, operated at CDS, Strasbourg, France.

References

- Balona L.A., 1977, MNRAS 84, 101 **BA77**
 Breger M., 1979, PASP 91, 5 **BR79**
 Breger M., 1995, PASPC 76, 596
 Cayrel de Strobel G., 1996, A&AR 7, 243
 Charbonneau P., 1993, ApJ 405, 720
 Claret A., 1995, A&AS 109, 441
 Crawford D.L., 1979, AJ 84, 1858
 Gray R.O., Olsen H.H., 1991, A&AS 87, 541
 Handler G., 1995, IBVS 4216
 Hauck B., Mermilliod M., 1990, A&AS 86, 107
 Kusakin A.V., Mkrtychian D.E., 1996, IBVS 4314 **KS96**
 Kuschnig R., Paunzen E., Weiss W.W., 1994a, IBVS 4069 **KU94a**
 Kuschnig R., Paunzen E., Weiss W.W., 1994b, IBVS 4070 **KU94b**
 Kuschnig R., Gelbmann M., Paunzen E., Weiss W.W., 1996, IBVS 4349 **KU96**
 Kuschnig R., Paunzen E., Weiss W.W., 1997, IBVS 4483 **KU97**
 Michaud G., Charland Y., 1986, ApJ 311, 326
 Napiwotzki R., Schönberner D., Wenske V., 1993, A&A 268, 653
 Paunzen E., 1995, IBVS 4254 **PA95c**
 Paunzen E., Duffee B., 1995, IBVS 4255 **PA95d**
 Paunzen E., Gray R.O., 1997, A&AS 126, 407
 Paunzen E., Handler G., 1996a, IBVS 4301 **PA96a**
 Paunzen E., Handler G., 1996b, IBVS 4318 **PA96b**
 Paunzen E., Weiss W.W., 1994, IBVS 3986 **PA94a**
 Paunzen E., Weiss W.W., North P., 1994, IBVS 4068 **PA94b**
 Paunzen E., Handler G., Weiss W.W., North P., 1994, IBVS 4094 **PA94c**
 Paunzen E., Heiter U., Weiss W.W., 1995, IBVS 4151 **PA95a**
 Paunzen E., Heiter U., Weiss W.W., 1995, IBVS 4191 **PA95b**
 Paunzen E., Weiss W.W., Heiter U., North P., 1997a, A&AS 123, 93
 Paunzen E., Kuschnig R., Handler G., Gelbmann M., Weiss W.W., 1997b, A&AS 124, 23
 Paunzen E., Heiter U., Handler G., et al., 1998a, A&A 329, 155 **PA98a**
 Paunzen E., Weiss W.W., Martinez P., et al., 1998b, A&A 330, 605 **PA98b**
 Renson P., Faraggiana R., Böhm C., 1990, Bull. Inform. CDS 38, 137
 Schmidt-Kaler Th., 1982, in: Landolt-Börnstein New Series, group VI, vol. 2b, p. 453
 Stellingwerf R.F., 1979, ApJ 227, 935
 Strassmeier K.G., Boyd L.J., Epand D.H., Granzer Th., 1997, PASP 109, 697
 Stürenburg S., 1993, A&A 277, 139
 Turcotte S., Charbonneau P., 1993, ApJ 413, 376
 Venn K.A., Lambert D.L., 1990, ApJ 363, 234
 Waelkens C., Rufener F., 1983, Hvar Obs. Bull. 7, 301 **WA83**
 Weiss W.W., Paunzen E., Kuschnig R., Schneider H., 1994, A&A 281, 797 **WE94**